EPJ Web of Conferences **292**, 10002 (2024) https://doi.org/10.1051/epjconf/202429210002
NRM2023

Noniterative finite amplitude methods for giant resonances and the application to the neutron radiative capture cross sections

Hirokazu Sasaki[1,*], *Toshihiko* Kawano[1], and *Ionel* Stetcu[1]

[1]Los Alamos National Laboratory, USA

Abstract. We calculate the electric dipole (E1) and the magnetic dipole (M1) giant resonances with noniterative finite amplitude methods and demonstrate how the fully microscopic density functional theory predicts the giant resonances without any phenomenological parameters. Then, we calculate neutron capture reactions based on the statistical Hauser-Feshbach theory with the result of E1 and M1 transitions and find that the capture cross sections for deformed nuclei are enhanced due to the contribution from the low energy M1 scissors mode.

1 Introduction

Giant resonances (GRs) are collective motions of nucleons inside the nucleus. Since the first measurement of the electric giant dipole resonance (GDR) in the photoabsorption experiments [1], various types of GRs were experimentally confirmed [2]. The strengths of GRs are applied to nuclear reaction theories, nuclear data evaluations, and stellar nucleosynthesis. In particular, neutron capture cross sections are calculated with the strengths of electric dipole (E1) and the magnetic dipole (M1) transitions under the Brink-Axel hypothesis [3] in the statistical Hauser-Feshbach theory [4, 5]. Since the production of large amounts of unstable nuclei, the calculated neutron capture cross sections are essential to the rapid neutron capture process (r-process) inside core-collapse supernovae and neutron-star mergers that can synthesize half of the heavy elements on the periodic table [6]. The capture reaction is also important for the neutrino-induced nucleosynthesis in core-collapse supernovae [7–10].

The fully microscopic density functional theory (DFT) is a contemporary theoretical approach to studying nuclear structures. Various GRs can be microscopically calculated with random-phase approximation (RPA) and the extended quasiparticle-RPA (QRPA) by considering pairing interactions [11, 12]. The finite amplitude method (FAM) [13, 14] is a feasible method to solve the self-consistent (Q)RPA equation and applied to various collective excitations such as multipole modes on photoabsorptions [15–19], β-decays [20, 21], and spontaneous fission [22].

In this paper, we overview the noniterative FAM developed in our previous works [18, 19] and show the results of giant resonances and the neutron capture cross sections for deformed nuclei.

*e-mail: hsasaki@lanl.gov

2 Methods

We briefly introduce the framework of the noniterative FAM and the derivation of RPA matrices. From the linear response of the time-dependent Hartree-Fock (TDHF) equation and the Fourier transform, the equations of forward and backward amplitudes of a frequency ω are given by [13, 16, 18]

$$(\epsilon_m - \epsilon_i - \omega)X_{mi}(\omega) + \langle\phi_m|\,\delta h(\omega)\,|\phi_i\rangle = -\langle\phi_m|\,V_{\rm ext}(\omega)\,|\phi_i\rangle\,, \quad (1)$$

$$(\epsilon_m - \epsilon_i + \omega)Y_{mi}(\omega) + \langle\phi_i|\,\delta h(\omega)\,|\phi_m\rangle = -\langle\phi_i|\,V_{\rm ext}(\omega)\,|\phi_m\rangle\,, \quad (2)$$

where $X_{mi}(\omega)$ and $Y_{mi}(\omega)$ are matrix components of forward and backward amplitudes, $\{\phi_i\}(i = 1, ..., A)$ and $\{\phi_m\}(m = A + 1, ...)$ are hole and particle states of the HF single-particle states, $\epsilon_{m/i}$ is the corresponding HF energy eigenvalue, $V_{\rm ext}(\omega)$ is the external field for collective motions, and $\delta h(\omega)$ is the residual interaction induced by the external field. We drop the index ω hereafter. The obtained forward and backward amplitudes from the above equations are applied to calculate transition strengths and cross sections of GRs.

One of the difficulties to solve Eqs. (1) and (2) is to calculate δh. FAM is an efficient way to calculate such a residual interaction. In the framework of FAM, the residual interaction is described with a small parameter η,

$$\delta h = \frac{1}{\eta}(h[\psi_i'^*, \psi_i] - h[\phi_i^*, \phi_i]), \quad (3)$$

$$\psi_i = \phi_i + \eta\sum_{m>A} X_{mi}\phi_m, \quad (4)$$

$$\psi_i'^* = \phi_i^* + \eta\sum_{m>A} Y_{mi}\phi_m^*, \quad (5)$$

where h is the TDHF Hamiltonian. In the conventional FAM, the residual interaction and amplitudes are calculated iteratively with Eqs. (1)-(5).

In the limit of $\eta \to 0$, the residual interaction in Eq. (3) is described by the linear combination of the forward and backward amplitudes [18],

$$\lim_{\eta\to 0}\delta h = \sum_{nj} X_{nj}\left.\frac{\partial h}{\partial(\eta X_{nj})}\right|_{\eta=0} + \sum_{nj} Y_{nj}\left.\frac{\partial h}{\partial(\eta Y_{nj})}\right|_{\eta=0}. \quad (6)$$

In such explicit linearization, we do not need any parameter η and iterative procedures to solve Eqs. (1)-(5) as done in the conventional FAM. Then, the RPA equation is derived from Eqs. (1), (2), and (6),

$$\left\{\begin{pmatrix} A & B \\ B^* & A^* \end{pmatrix} - \omega\begin{pmatrix} 1 & 0 \\ 0 & -1 \end{pmatrix}\right\}\begin{pmatrix} X_{nj} \\ Y_{nj} \end{pmatrix} = -\begin{pmatrix} f_{mi} \\ f_{im} \end{pmatrix}, \quad (7)$$

$$A_{mi,nj} = (\epsilon_m - \epsilon_i)\,\delta_{mn}\delta_{ij} + \int {\rm d}^3r\,\phi_m^*\left(\frac{\partial h}{\partial(\eta X_{nj})}\right)_{\eta=0}\phi_i\,, \quad (8)$$

$$B_{mi,nj} = \int {\rm d}^3r\,\phi_m^*\left(\frac{\partial h}{\partial(\eta Y_{nj})}\right)_{\eta=0}\phi_i\,, \quad (9)$$

$$f_{mi} = \int {\rm d}^3r\,\phi_m^* V_{\rm ext}\phi_i, \quad f_{im} = \int {\rm d}^3r\,\phi_i^* V_{\rm ext}\phi_m, \quad (10)$$

where the components of RPA matrices A and B are calculated with the linearization of the Skyrme potentials. The detailed descriptions of these matrices are given in Ref. [18].

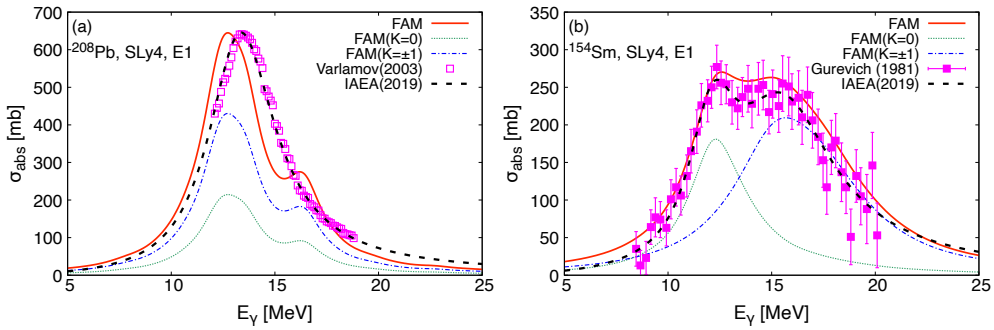

Figure 1. The GDR cross sections for (a)^{208}Pb and (b)^{154}Sm. The solid line shows the result of the noniterative FAM. The dotted and dash-dotted lines show the partial contributions from $\mathrm{d}B(E_\gamma, D_0)/\mathrm{d}E_\gamma$ and $\sum_{K=\pm1} \mathrm{d}B(E_\gamma, D_K)/\mathrm{d}E_\gamma$. The symbols are both the reported and evaluated experimental data [25, 26]. The dash line is the evaluated GDR cross section [27].

The above discussion can be extended to the framework of QRPA with the HF+BCS single-particle states by multiplying a BCS parameter such as $\zeta^\tau_{\mu\nu} = u_\nu v_\mu + \tau u_\nu v_\mu$ by the operators [19]. Such extension from RPA to QRPA is needed for the calculation of the M1 transition for open-shell and deformed nuclei. We calculate both E1 and M1 transitions for even-even nuclei based on the noniterative FAM-QRPA with SLy4 Skyrme interactions [23].

The photoabsorption cross sections obtained in the microscopic calculations are applied to the neutron capture cross sections through the statistical Hauser-Feshbach model. The calculation is carried out with the coupled channels Hauser-Feshbach code $\mathrm{CoH_3}$ [24]. The calculated photoabsorption cross sections $\sigma_{\mathrm{abs}}(E_\gamma; XL)$ $(X = E, M, L = 1)$ are used for the γ–ray strength function,

$$f_{XL}(E_\gamma) = \frac{\sigma_{\mathrm{abs}}(E_\gamma; XL)}{(2L+1)\pi(\hbar c)^2 E_\gamma^{2L-1}}, \tag{11}$$

where E_γ is the energy of the emitted photon from the compound nucleus. The γ–ray strength function is used to calculate the γ–ray transmission coefficient in the statistical model.

3 Results and Discussions

Figure 1 shows the FAM-QRPA results of GDR cross sections for ^{208}Pb and ^{154}Sm. We employ the E1 operator $D_K(K = 0, \pm1)$ [18] in Eq. (10) with Im ω=62.5 keV. We adjust the values of peak cross sections with a convolution of a Lorentzian function. The calculation results (solid lines) reproduce well the resonance energies of the evaluated cross sections (dashed lines) within 0.6 MeV. We remark that such a calculated resonance energy is almost independent of the choice of the Lorentzian width in the convolution. The partial contributions from different $K(= 0, \pm1)$ in the E1 operator are shown in the dotted and dash-dotted lines. The dash-dotted line in Fig. 1(a) is completely twice the dotted line because ^{208}Pb is a spherical nucleus and the transition strength is independent of the value of K. On the other hand, the GDR peak splits into two for deformed nuclei such as ^{154}Sm. The FAM results in Fig. 1(b) reproduce such a split of the GDR. The energy-weighted sum rule m_1 [17, 18] computed from both the integration of $\sigma_{\mathrm{abs}}(E_\gamma; E1)$ and the HF ground-state density is consistent within a few percent for ^{208}Pb and ^{154}Sm.

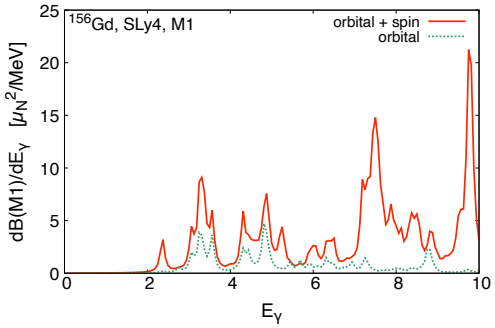

Figure 2. The transition strengths of the M1 transitions for ^{156}Gd. The solid (dotted) line shows the result with (without) the contribution from the spin-flip transition.

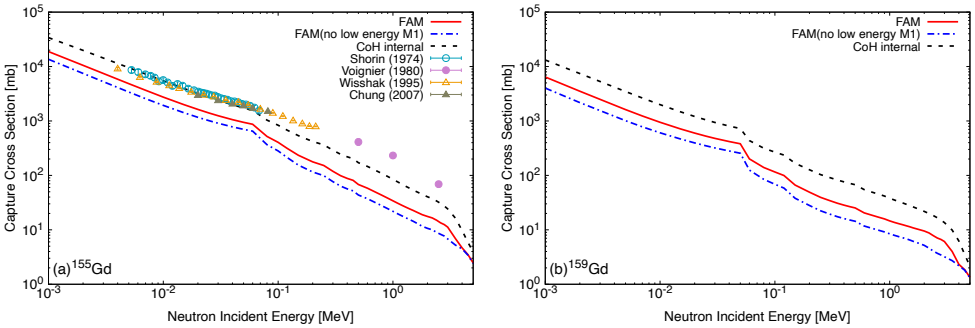

Figure 3. The neutron capture cross sections on (a)^{155}Gd and (b)^{159}Gd. The solid line shows the result with FAM photoabsorption cross sections ($XL = E1, M1$) in Eq. (11). The dash-dotted line shows the result without the contribution from the M1 transition lower than 4 MeV. The dashed line shows the result with the internal γ–ray strength functions in CoH_3, which are phenomenologically parameterized giant resonances. The symbols are experimental data [30–33].

Figure 2 shows the results of the M1 transition strengths for ^{156}Gd with and without the spin g factor in the M1 operator that includes both spin and orbital angular momentum operators. The spin-flip transition dominantly occurs in $E_\gamma \geq 5$ MeV and the contribution from the orbital motion is prominent at low energies. Such low energy M1 transition associated with the orbital operator can be seen as a scissors mode induced by the collective motions of nucleons inside a deformed nucleus. The scissors mode appears around 3 MeV and the total strength is $\sum B(M1) \sim 3\mu_N^2$ for rare-earth nuclei [28]. We obtain $\sum B(M1) = 4.9\mu_N^2$ by integrating the solid line in Fig. 2 up to 4 MeV. This overestimation can be improved by introducing the quenching of the spin g factor [29] in the M1 operator.

Figure 3 shows the calculated neutron capture cross sections for ^{155}Gd and ^{159}Gd compared with experimental data. There is no experimental data for ^{159}Gd due to an unstable nucleus. The properties of the calculated cross sections are similar for both stable and unstable Gd isotopes. For the calculation of the γ–ray strength function in Eq. (11), we employ the FAM results of the E1 and M1 transitions for ^{156}Gd and ^{160}Gd. The calculated capture cross sections are sensitive to the strength functions at low energies. The dash-dotted lines

are lower than the solid lines, which indicates the enhancement induced by the low energy M1 scissors mode ($E_\gamma \leq 4$ MeV). The contribution from the M1 scissors mode is discussed with the average γ–ray width $\langle\Gamma_\gamma\rangle$ [19] and the M1 scissors mode contributes to about half of the total calculated cross section. The calculated capture cross section with the FAM result is lower than the dashed line and experimental data in Fig. 3(a). Such a discrepancy can be improved by microscopic calculations beyond QRPA such as quasiparticle-phonon model (QPM) [34] and quasiparticle time blocking approximation (QTBA) [35]. Such advanced theoretical frameworks can induce fragmentation of the E1 transition strength to the low energy tail of GDR and enhance the γ-ray strength function at low energies. The pygmy dipole resonance (PDR), which appears near and below the neutron separation energy impacts both the γ–ray strength function and the neutron capture cross section [34, 36, 37]. The strength of PDR in a nucleus with neutron excess is also important for constraining the electric dipole polarizability [38, 39] and the neutron skin [40].

4 Conclusion

We rederive the (Q)RPA equation based on the noniterative FAM and calculate the E1 and M1 photoabsorption cross sections. The FAM calculation reproduces well the resonance energies of GDRs for heavy nuclei without any phenomenological parameters. For the M1 transition, we confirm both spin-flip transitions in the 5 to 10 MeV excitation energy and the contribution from orbital motions at low energies where the M1 scissors mode was observed in nuclear experiments. We apply the FAM result of E1 and M1 transitions to the calculation of neutron capture cross sections for deformed gadolinium isotopes in the statistical Hauser-Feshbach model. The M1 scissors mode can contribute to about half of the capture cross sections. The underestimation of the calculated cross section could be improved by considering the uncertainty of low energy E1 transitions neglected in the framework of QRPA.

References

[1] W. Bothe, W. Gentner, Zeitschrift fur Physik **106**, 236 (1937)
[2] M. Harakeh, A. Woude, *Giant Resonances: Fundamental High-frequency Modes of Nuclear Excitation* (Oxford University Press, 2001), ISBN 9780198517337
[3] D.M. Brink, unpublished D. Phil. thesis, Oxford University (1955)
[4] W. Hauser, H. Feshbach, Phys. Rev. **87**, 366 (1952)
[5] M.R. Mumpower, T. Kawano, J.L. Ullmann, M. Krtička, T.M. Sprouse, Phys. Rev. C **96**, 024612 (2017)
[6] M.R. Mumpower, R. Surman, G.C. McLaughlin, A. Aprahamian, Prog. Part. Nucl. Phys. **86**, 86 (2016)
[7] H. Sasaki, T. Kajino, T. Takiwaki, T. Hayakawa, A.B. Balantekin, Y. Pehlivan, Phys. Rev. D **96**, 043013 (2017)
[8] H. Sasaki, Y. Yamazaki, T. Kajino, M. Kusakabe, T. Hayakawa, M.K. Cheoun, H. Ko, G.J. Mathews, Astrophys. J. **924**, 29 (2022)
[9] H. Sasaki, Y. Yamazaki, T. Kajino, G.J. Mathews, arXiv:2307.02785 (2023)
[10] H. Ko, D. Jang, M.K. Cheoun, M. Kusakabe, H. Sasaki, X. Yao, T. Kajino, T. Hayakawa, M. Ono, T. Kawano et al., Astrophys. J. **937**, 116 (2022)
[11] P. Ring, P. Schuck, *The Nuclear Many-Body Problem*, Physics and astronomy online library (Springer, 2004), ISBN 9783540212065
[12] D. Rowe, *Nuclear Collective Motion: Models and Theory* (World Scientific, 2010), ISBN 9789812790644

[13] T. Nakatsukasa, T. Inakura, K. Yabana, Phys. Rev. C **76**, 024318 (2007)
[14] P. Avogadro, T. Nakatsukasa, Phys. Rev. C **84**, 014314 (2011)
[15] M. Kortelainen, N. Hinohara, W. Nazarewicz, Phys. Rev. C **92**, 051302 (2015)
[16] T. Inakura, T. Nakatsukasa, K. Yabana, Phys. Rev. C **80**, 044301 (2009)
[17] T. Oishi, M. Kortelainen, N. Hinohara, Phys. Rev. C **93**, 034329 (2016)
[18] H. Sasaki, T. Kawano, I. Stetcu, Phys. Rev. C **105**, 044311 (2022)
[19] H. Sasaki, T. Kawano, I. Stetcu, Phys. Rev. C **107**, 054312 (2023)
[20] E.M. Ney, J. Engel, T. Li, N. Schunck, Phys. Rev. C **102**, 034326 (2020)
[21] N. Hinohara, J. Engel, Phys. Rev. C **105**, 044314 (2022)
[22] K. Washiyama, N. Hinohara, T. Nakatsukasa, Phys. Rev. C **103**, 014306 (2021)
[23] E. Chabanat, P. Bonche, P. Haensel, J. Meyer, R. Schaeffer, Nucl. Phys. A **635**, 231 (1998)
[24] T. Kawano, European Physical Journal A **57**, 16 (2021)
[25] V.V. Varlamov, M.E. Stepanov, V.V. Chesnokov, Bull.Russian Academy of Sciences - Physics **67**, 724 (2003)
[26] G.M. Gurevich, L.E. Lazareva, V.M. Mazur, S.Y. Merkulov, G.V. Solodukhov, V.A. Tyutin, Nuclear Physics, Section A **351**, 257 (1981)
[27] T. Kawano, Y. Cho, P. Dimitriou, D. Filipescu, N. Iwamoto, V. Plujko, X. Tao, H. Utsunomiya, V. Varlamov, R. Xu et al., Nucl. Data Sheets **163**, 109 (2020)
[28] A. Richter, Prog. Part. Nucl. Phys. **34**, 261 (1995)
[29] G. Kružić, T. Oishi, D. Vale, N. Paar, Phys. Rev. C **102**, 044315 (2020)
[30] V.N. Kononov, B.D. Yurlov, G.N. Manturov, E. Poletaev, V.M. Timokhov, V.S. Shorin, Yadernye Konstanty **22**, 29 (1977)
[31] J. Voignier, S. Joly, G. Grenier, D.M. Drake, L. Nilsson, Centre d` Etudes Nucleaires, Saclay Reports p. 5089 (1981)
[32] K. Wisshak, F. Voss, F. Käppeler, K. Guber, L. Kazakov, N. Kornilov, M. Uhl, G. Reffo, Phys. Rev. C **52**, 2762 (1995)
[33] J. Nishiyama, T.I. Ro, M. Igashira, W.C. Chung, G. Kim, T. Ohsaki, S. Lee, T. Katabuchi, *International Conference on Nuclear Data for Science and Technology* (2007)
[34] N. Tsoneva, S. Goriely, H. Lenske, R. Schwengner, Phys. Rev. C **91**, 044318 (2015)
[35] A. Avdeenkov, S. Goriely, S. Kamerdzhiev, S. Krewald, Phys. Rev. C **83**, 064316 (2011)
[36] S. Goriely, Phys. Lett. B **436**, 10 (1998)
[37] E. Litvinova, H.P. Loens, K. Langanke, G. Martinez-Pinedo, T. Rauscher, P. Ring, F.K. Thielemann, V. Tselyaev, Nucl. Phys. A **823**, 26 (2009)
[38] J.L. Friar, Phys. Rev. C **16**, 1540 (1977)
[39] A.P. Tonchev et al., Phys. Lett. B **773**, 20 (2017)
[40] N. Tsoneva, H. Lenske, Phys. Rev. C **77**, 024321 (2008)